

Measuring the speed of a surface plasmon

M. Bai, C. Guerrero, S. Ioanid, E. Paz, M. Sanz, and N. García

Laboratorio de Física de Sistemas Pequeños y Nanotecnología, Consejo Superior de Investigaciones Científicas, Serrano 144 Madrid 28006, Spain

(Received 25 March 2003; revised manuscript received 17 December 2003; published 19 March 2004)

This paper presents experiments using an 800-nm pulsed laser and a streak camera with 2-ps resolution, which is implemented with a two-fiber differential measurements permitting a 0.2-ps resolution. With this technique, we measure the speed of the propagation of the surface plasmons. This velocity was found to be approximately $(0.57 \pm 0.19)c$, about 61% the value expected from simple theory (i.e., about $0.94c$). The former result may clarify what is going on at the metal vacuum interface excitations, and has been measured by a direct method without the need for any theory.

DOI: 10.1103/PhysRevB.69.115416

PACS number(s): 78.47.+p, 73.20.Mf, 68.37.Uv

Surface plasmons (SP's) are longitudinal collective electron oscillations at the interface between a metallic and a dielectric material.¹ A high sensitivity to the interface structure and composition, and also the significant enhancement of the local electromagnetic field, make SP spectroscopy a prospective interface and surface analysis tool.^{2,3} Also, second-harmonic generation has been observed.⁴ The SP technique has been combined with time-resolved laser spectroscopy^{5,6} in order to study the surface dynamics and associated ultrafast process on the surface region. Some time-resolved investigations have been carried out to get a better understanding about SP dynamics at the surface of thin metal films,⁷ and of metal nanostructures.^{8,9} On the other hand, ps time-resolved measurements of interferences with a few photons is possible by using a femtosecond pulsed laser combined with a streak camera with ps resolution.¹⁰ SP's have been also observed using charged particles.¹¹ The alteration on the propagation mode of the electromagnetic field, from the field inside a metal thin film and above the interface as a SP, spark our interest in the special optical properties at the metal surface, as well as the way it affects the propagation of the SP. This problem is also important to understand the group velocity and propagation in dispersive media and metals.¹² In order to clarify these points, it will be of value to know the speed of propagation of surface plasmons.

This paper presents experiments using a pulsed laser and a streak camera to measure the speed of propagation of the surface plasmons excited on the attenuated total reflection (ATR) configuration. The speed was found to be approximately $0.57c$ (c being the speed of light in vacuum) for an 800-nm wavelength, i.e., about 61% of $0.94c$, expected from the existing theory, or 62% of $0.92c$, obtained from a crude estimation in SP resonance experiments. This result is important because it may clarify what is going on at the metal vacuum interface excitations, and has been measured by using a direct method.

There is a strong field enhancement near the metal surface at the surface plasmon resonance,^{2,3} which implies a highly localized state at the surface, suggesting that the SP field propagation velocity can be different from that of light in the vacuum, even if most of the SP field propagation occurs there. Specifically, most of the plasmon energy lies in the vacuum above the metal surface within a few hundred na-

nometers. The phase and group propagation velocities— v_p and v_g , respectively—are classically defined by

$$v_p = \frac{\omega}{k}, \quad v_g = \frac{d\omega}{dk}, \quad (1)$$

where k and ω are the wave vector and the radiation frequency, respectively. In particular, for the case of an Ag thin film, where the imaginary part ε_2 of the dielectric function is much less than the real part ε_1 , and therefore may be neglected, the dispersion relation for a SP at the metal-vacuum interface is [Eq. (2.4) in Ref. 1]

$$k_x = \frac{\omega}{c} \sqrt{\frac{\varepsilon_1}{\varepsilon_1 + 1}}. \quad (2)$$

We notice that the phase velocity $v_p = c \times \sqrt{(1 + \varepsilon_1)/\varepsilon_1}$ is slightly less than the speed of light in vacuum c , since ε_1 is negative and $|\varepsilon_1| \gg 1$. Utilizing $\varepsilon_1 = \varepsilon_1(\omega)$ data for Ag by Johnson and Christy,¹³ the group velocity v_g is determined to be also slightly smaller than c . In our experimental setup, using 800-nm wavelength (1.55-eV photon energy), we get from experiments¹³ ε_1 , $v_p = 0.98c$, and $v_g = 0.94c$.

This theory for surface plasmons and its dispersion relation is based on the discontinuity of the dielectric constant at the metal-vacuum interface, and predicts the positions of the surface resonances in the reflectivity by fitting the dielectric constant of the metal. This does not, however, imply that it will describe the dynamic aspects such as the speed of plasmon propagation because this excitation has a tail at the metal portion of the interface and another at the vacuum. Inside the Ag thin film, the field propagation is very complicated because of the negative dielectric constant. Using Eq. (1), we calculate that the phase and group velocity in the metal thin film are much smaller than the speed of light in air, being approximately $0.18c$ and $0.09c$, respectively. There is, therefore, considerably different field propagation around the interface due to the difference in propagation in the metal and in vacuum. In other words, it suggests that the group velocity of a SP in the surface regime can be different from in the metal as well as in the vacuum. It would be interesting to have a direct method of measuring the speed of a surface plasmon, independent of theory, since it will pro-

vide information about the dielectric function in the transition region between bulk and vacuum.

We first examine the SP excitation condition and the field propagation in the well-known ATR configuration. Furthermore, we take measurements in the time domain for the SP propagation in the near-field region with a picosecond time-resolved method, and then detect the propagation speed of a SP. In our experiments, SP's are excited in a prism coupling, known as the ATR arrangement.¹⁴ Wave-vector matching to the mode at the silver-air interface in a prism-silver-air system is achieved when a *p*-polarized laser radiation is incident on the silver film at a certain angle just above the prism's critical angle; i.e., the incident wave in the metal slab is an attenuated wave. The sample is prepared by depositing 50 nm of silver on the hypotenuse face of a right angle BK7 glass prism ($n=1.515$ at 633 nm, $n=1.511$ at 800 nm), mounted on a rotation platform, thus allowing a fine-tuning of the angle of incidence.

The nature of the SP is a nonradiative electromagnetic (EM) mode, which is highly localized at the metal/air interface, typically within hundreds of nanometers above the surface. Near-field microscopy has, therefore, proved to be a good technique for SP measurement.^{15,16} In our experiment, we performed a one-dimensional constant height scan, utilizing a cut multimode fiber as a probe into the SP field, located just at the surface of the metal. The fiber was on a triaxial fiber positioner, which controlled the location of the spot on the sample. Through the well-known photon tunneling effect, the SP field was coupled into the optical fiber probe and then delivered and collected into the detector as the signal, proportional to the near-field intensity. The core diameter, however, of the fiber probe used was $51\ \mu\text{m}$, i.e., enough to check the SP intensity distribution through the whole beam region on the surface. The excitation source was a Ti-sapphire laser 800 nm in wavelength. The light signal was then sent to the photomultiplier tube (PMT) detector, so that we could record the intensity at each point in the scanning path, as shown in Fig. 1(a). In this way, we could obtain the intensity distribution profile of the evanescent field on the metal surface.

By examining the SP excitation with different lasers (1.55 and 1.96 eV), we recorded the reflected intensity around the SP resonance angle, as shown in Fig. 1(b). It has been verified that the SP resonance is very sensitive to the angle of incidence of the beam, and that the resonance angle changes according to the different incident photon energy. This implies that the plasmons are not degenerated (except in the asymptotic value k_x tending to infinity), but depend critically on the wave vector k_x parallel to the interface [Eq. (2)]. This is consistent with results from previous work on SP.¹

Moreover, we examined the field distribution profile of the SP's with a one-dimensional scan, controlling the fiber probe position just on the metal-air surface. From Figs. 2(a) and 2(b), we notice that the profile width of the SP is larger than the width of the profile for the incident beam, both for the case of an unfocused beam and for a focused beam. Along the propagation, there always exists a tail out of the excitation region by the incident beam, which is a clear indication of the SP's propagating on the surface.¹⁶ Also, in the

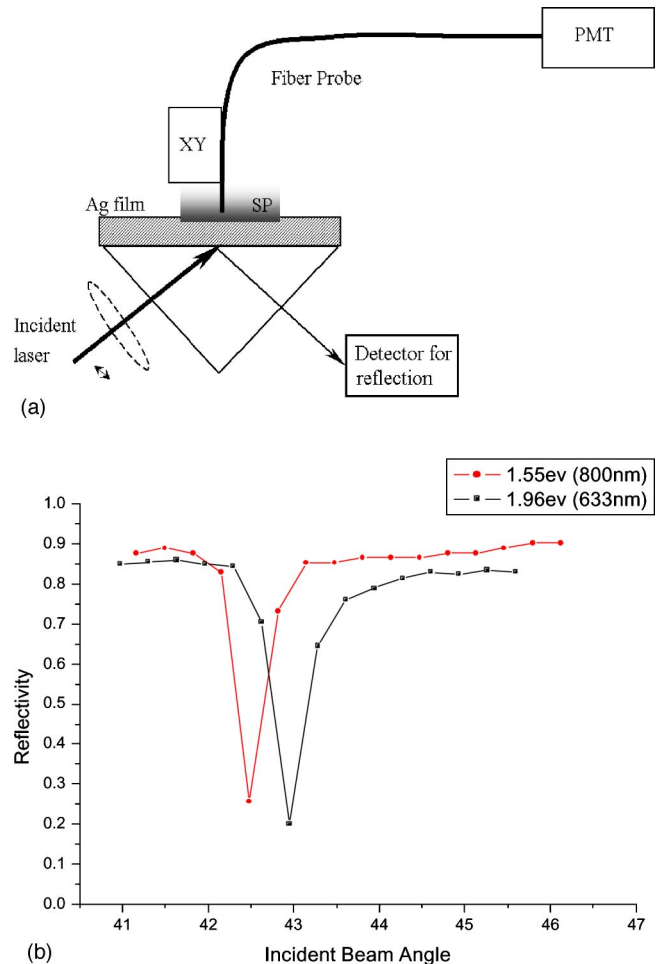


FIG. 1. (a) Schematic drawing of setup for the SP's intensity distribution measurement. (b) Reflected intensity vs angle of incidence for different wavelength lasers: 1.96 eV (633 nm) and 1.55 eV (800 nm).

SP resonance condition, the intensity of the near field is 150 times larger than out of the resonance. The minor fluctuation of the SP curve is due to small-scale topographic inhomogeneities in the metal film. A similar image of surface-plasmon propagation is also obtained with a continuum He-Ne laser.

In order to trace the propagation of the SP in the time domain, we set our streak camera in the operate mode for time-resolved measurements with two optical fibers (of the same length) for signal input (see Ref. 10 for more detailed explanations of the technique). The time-resolved experiment scheme is shown in Fig. 3. A beam splitter is placed in the incident beam path, one of the two split beams is coupled into the fixed fiber, and the other beam is sent to the prism for SP excitation. The fixed fiber serves as a reference, and the other is used to scan the Ag surface along the direction of the SP propagation. The latter scanning was performed for time measurements and the time differences between two fiber measurements gave us the resolution for the measurements. As we demonstrated in Fig. 6, for a given constant pulse shape, we can measure a shift in the pulse position that is much less than its width. This differential measurement permits a 0.2-ps resolution even if the streak camera has 2-ps resolution. Notice that this is a good enough resolution con-

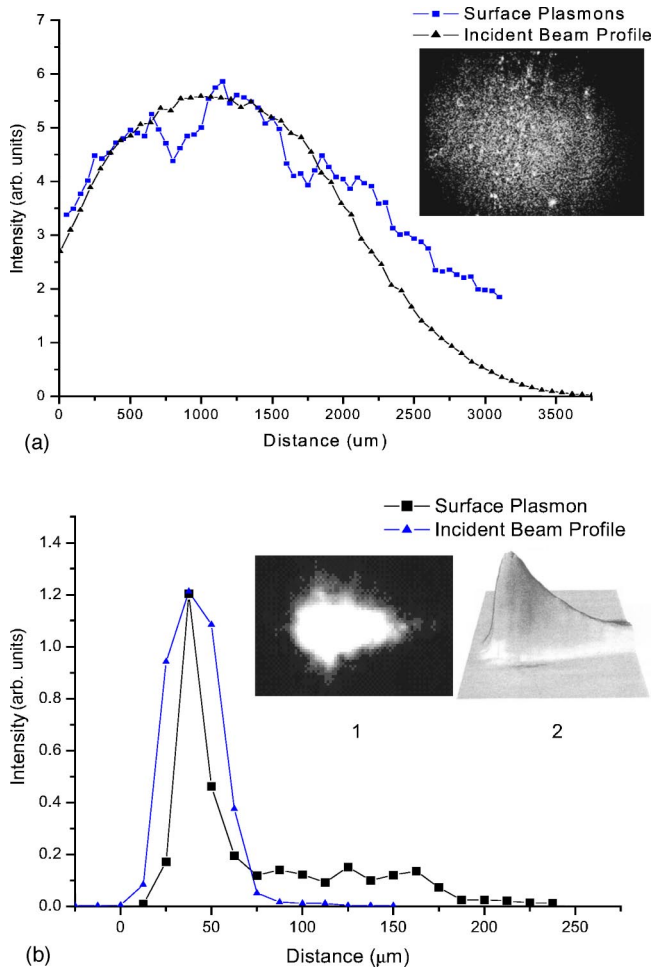


FIG. 2. Intensity profiles of the SP field in the direction of propagation, compared with the intensity profile of the incident laser beam profile. (a) From a nonfocused beam. (b) From a focused beam. The inset image 1 is the scattered SP distribution as observed by far-field microscopy. The elongated shape is due to the plasmon propagation. It is similar to the inset image 2, which is measured by the near-field method (Ref. 16).

sidering a 6-ps range of the measurement.

Figure 6 describes how the timing experiments are done and how the time values are extracted from the streak camera. For that, two synchronized signals are sent to the camera; one goes directly to the beam splitter and has a 10-ps width, while the other is the signal registered from a point at the SP. The first measurement is for the point marked “0” in Fig. 5(a). This difference in time is plotted in Fig. 6, “0” (upper panel). The next measurement is, for example, for point “1” in Fig. 5(a) and is plotted in Fig. 6, “1” (medium panel) and so on for point “2” and all the other points. From the difference in the time between the maximum of the time curves provided by the streak camera, we obtain the propagation times for the SP plotted in Fig. 5. There is very little indetermination (less than 0.2 ps) in these measurements, because the maxims are determined by the values at which the derivatives of the curves in Fig. 6 are zero.

Being limited by the 2-ps resolution of the streak camera, we could not distinguish the time of the propagation from a

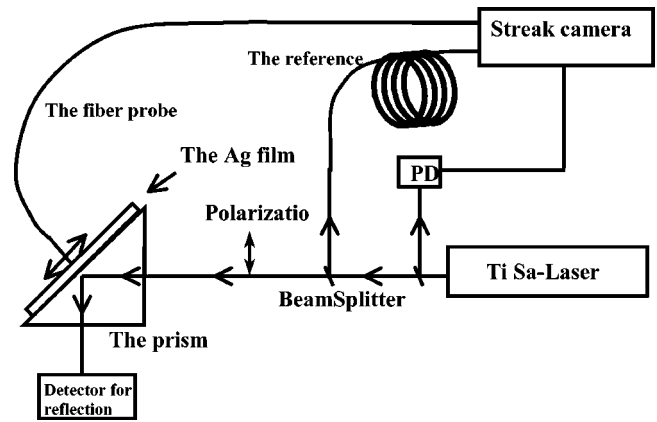


FIG. 3. Schematic representation of the time-resolved measurement experiments on the propagation of the SP's.

single fiber involved in the experiments, which is the reason for the setup of Fig. 3. It was, furthermore, necessary that the SP have propagation lengths (L) of the order of $200 \mu\text{m}$ or larger. The latter value is given by $L = \frac{1}{2} \text{Im}(k_x)$. Figure 4 shows the plot values of L versus wavelength for the dielectric constant values obtained by Johnson and Christy,¹³ taking into account the relative data error range. As is well known, these values of L are very dependent on the wavelength of the radiation. These also varied according to whether the SP propagates in a large surface area or in a striped region.¹⁷ At 800 nm, there is an indetermination because of the experimental errors in defining the permittivity, but it is clear that the values of L are much greater than those at wavelengths smaller than 633 nm, where other experiments have been performed.¹⁷ We also notice that a SP length of $150 \mu\text{m}$ on silver film has been obtained with a 785-nm laser excitation.¹⁷ In our time-resolved measurements, out of the total measured range, apparent SP propagation occurs along about 600- μm length (Fig. 5). However, taking into account the intensity decay, when it reaches $1/e$,

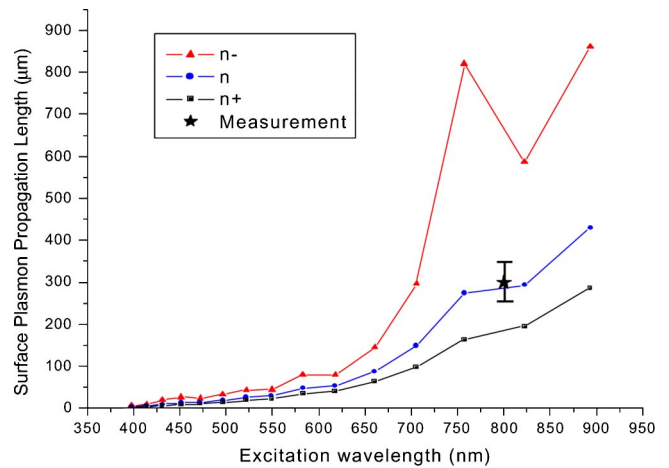


FIG. 4. SP propagation length vs excitation wavelength. Lines are calculated applying Johnson and Christy's Ag constant, taking into account the error of the real part n of the metal constants. The star with the error bar marks the measured SP propagation length in our time-resolved experiment.

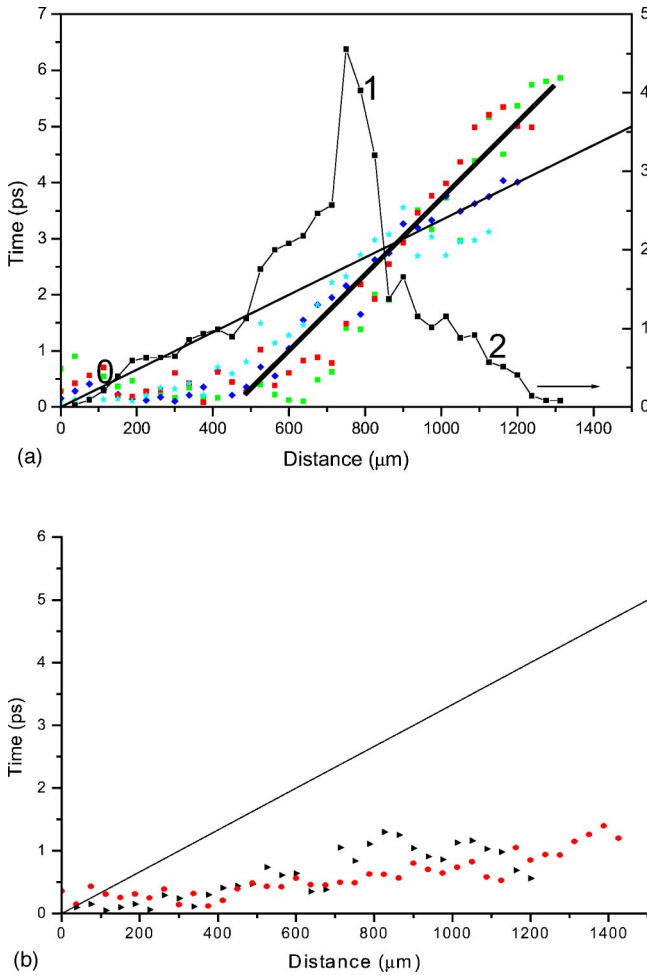


FIG. 5. (a) Time-resolved measurements of the time position changes along the direction of the SP's propagation. Dots represent time positions along the propagation. The speed of light in vacuum (thinner straight line) and the velocity of the SP (thicker straight line) on the surface are indicated. The corresponding intensity profile is also superimposed in the image. (b) The time-resolved measurement for the out-of-SP condition, with the straight line indicating the speed of light in vacuum. In this case, no propagation is observed.

the propagation length L is roughly estimated as $\sim 300 \mu\text{m}$ (indicated by the star in Fig. 4). Nevertheless, this is within the range of the calculated values. We also performed experiments for 400 nm at the double frequency of the IR laser, but the values of L were much smaller and no measurements could be performed with precision. From the above it is evident that our time resolution measurements of L are within the range predicted by theory.

In the experiment, the fiber probe scans on the surface along the direction of propagation of the SP. In order to obtain the corresponding timing value, the time difference between the coupled SP signal from the scanning fiber and the reference one was recorded in the same snapshot of the streak camera. Along the path of propagation, the corresponding time increases, indicating the propagation of the SP in the time domain.

In Fig. 5(a), we plotted the obtained time versus the dis-

tance data, recorded from the streak camera with the fiber registering intensity from different points in the surface (see Fig. 6 for more explanation). With reference to the guidance line, we estimated that the velocity of the SP is about $0.57c$. This is less than the estimated group velocity $v_g = 0.94c$ in the metal-air interface but larger than that in the metal, $v_g = 0.09c$. It is noteworthy that the dispersion relation Eq. (2) we used to estimate the group velocity is derived for the smooth surface of a semi-infinite metal with dielectric constant ϵ_1 , adjacent to a medium ($\epsilon_2 = 1$ as air). The dispersion relation may not be precisely correct for metal films with finite thickness, especially when that thickness is very small ($k_{z1}d \ll 1$). In that case, the interaction of the EM field on both surfaces will change the SP frequency (Ref. 1, p. 25). We draw our attention to two facts, however. First is the fact that we are dealing with a metal film with a thickness of 50 nm, and the SP's penetration depth into the silver is ~ 23 nm for an 800-nm laser wavelength ($k_{z1}d = 2$). The second fact is that we have an asymmetric ATR setup, so the SP is excited only on the surface adjacent to the air, and the coupling between the two surfaces, if there exists any, is very weak. Taking into account all of the above, we would say in this case that Eq. (2) is a very good approximation. Nevertheless, we can make a direct estimation of the group velocity v_g utilizing the experimental data in Fig. 1(b), from which we get resonance condition k_{SP1} and k_{SP2} with corresponding ω_1 and ω_2 . Roughly the group velocity is thus estimated as

$$v_g \approx \left(\frac{\omega_1 - \omega_2}{k_{SP1} - k_{SP2}} \right) = 0.92c,$$

which is not much different from the estimation based on Eq. (2).

However, this result is consistent with the assumption that for a SP, the group velocity (which represents the energy flow) near the surface should be a tradeoff between the decay length in the metal and the air. For comparison, we also performed the same measurements for a transmitted total reflection field out of the SP resonance condition [Fig. 5(b)]. Within the 2-ps limits of our camera resolution, the time position does not show any obvious increase in the direction of propagation. This means that at all points of the surface, the radiation occurs at the same time. Therefore, there is no time delay between different points at the surface. However, the SP is a highly localized EM mode, and the field propagates at and above the metal surface. This result is consistent with the length of decay of the electromagnetic field associated with the SP from the interface into each of the bounding media. On the metal side, the $1/e$ field decay length is typically ~ 20 nm but it increases to hundreds of nanometers in the air.

The result obtained for the group velocity is new. The SP wave function has part of its weight in the metal where the estimated group velocity is $0.09c$, and part in the air where the value is c . The obtained experimental value is, therefore, not unreasonable. Furthermore, even if the static properties of SP are more or less described by the model used above, that does not mean that the same thing would happen for the dynamic properties, such as the speed of SP propagation.

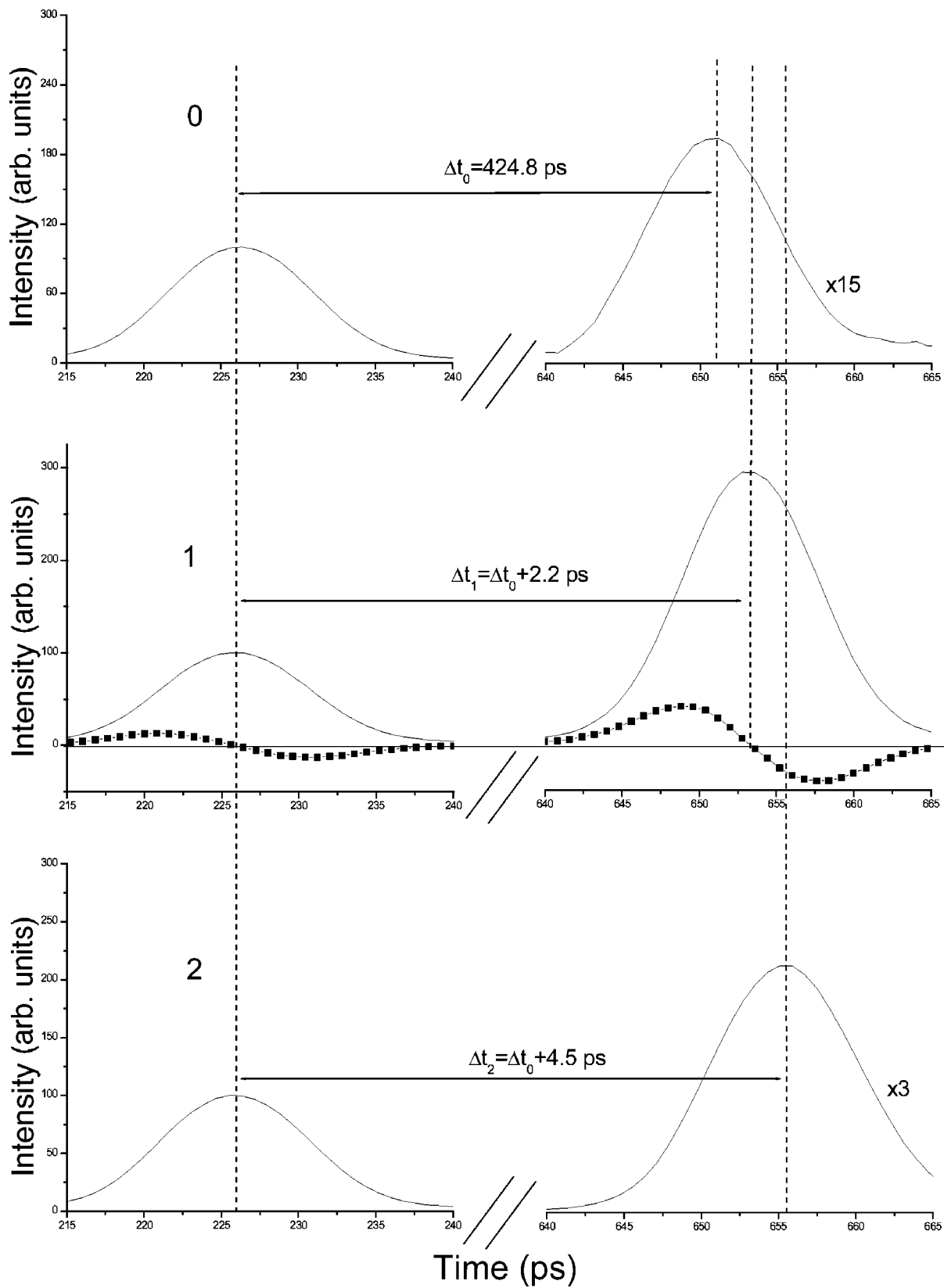


FIG. 6. Demonstration for SP propagation timing measurement. The laser pulse through the reference fiber (left) and the coupled SP signal through the scanning fiber (right) are recorded by streak camera. Δt is the measured time difference between them. We obtain Δt by taking the values at which the derivatives of the curves (indicated by lines with squares) are zero, as shown in the middle panel for point “1.” The numerical errors in Δt are about 0.2 ps. The shifts of Δt values between points represent the SP propagation in time. The temporal profiles of “0,” “1,” and “2,” correspond to the data points marked in Fig. 5(a).

This, in fact, is what our experiment reveals. In addition, it is clear that a model which considers a discontinuity of the dielectric constant at the metal surfaces cannot be right no matter what. We know that this value has to evolve smoothly from inside the metal to the air. It should be a function of the distance to the surface. Nevertheless, this could be a result of thin-film aging, surface roughness, or multiscattering effects. It should be said, however, that the result reported is well described on average by several samples that have been measured.

To get some understanding of the new physics provided by the experiment, and to interpret the group velocity behavior around the interface, we introduce an effective dielectric constant ε_{eff} around the interface, defined by the contribution from SP field flow above the interface and the field flow under the interface, as described in the following:

$$\varepsilon_{\text{eff}} = \frac{\varepsilon_0 \int_0^{\infty} e^{-k_{z0}z} dz + \varepsilon_1 \int_0^{\infty} e^{-k_{z1}z} dz}{\int_0^{\infty} e^{-k_{z0}z} dz + \int_0^{\infty} e^{-k_{z1}z} dz}. \quad (3)$$

Here ε_0 and ε_1 are the dielectric constants in air and in the metal, and k_{z0} and k_{z1} are the wave vector in air and in metal, respectively, with regard to the wave-vector relation,

$$k_{z1} = \sqrt{|\varepsilon_1|} k_{z0}. \quad (4)$$

Applying our experimental conditions to Eq. (3), i.e., $\varepsilon_0 = 1$ and $\varepsilon_1 = \varepsilon_{\text{Ag}}$, we obtain $\varepsilon_{\text{eff}} = -3.79$ from Eqs. (1) and (2). This effective optical constant around the transition region of a metal surface, which is supposed to be much different from that corresponding to the air and the metal, gives us a new way to describe the properties of the interface. This model tries to take into account a smooth variation of the dielectric constant in a crude way. But there are other effects that should be considered, such as nonlocality. In addition to this, surface aging, oxidation (even if the Ag is capped with 1 nm of Au), and a roughness of approximately 5 nm in height as measured by scanning tunneling microscopy should have some influence on the SP velocity.

In conclusion, we have examined the SP excitation condition and have imaged the field propagation in an ATR schematic for an Ag metal thin film. We took measurements in the time domain for the SP propagation in the near-field region with a 0.2 resolution using a two-fiber differential measurement with a time-resolved streak camera. An effective dielectric constant around the transition-metal surface is proposed to interpret the measured field group velocity of the surface plasmon. The measured SP's speed is $(0.57 \pm 0.19)c$, i.e., 61% of the value of $0.94c$ predicted by the existing theory.

This work has been supported by the Spanish DGICYT.

¹H. Raether, *Surface Plasmons on Smooth and Rough Surfaces and on Gratings*, Springer Tracts in Modern Physics Vol. 111 (Springer-Verlag, Berlin, 1988).

²H. Raether, *Surf. Sci.* **8**, 233 (1967); G. Diaz, N. García, and H. Raether, *ibid.* **146**, 1 (1984).

³N. García, *Opt. Commun.* **45**, 307 (1983); N. García, G. Diaz, J. H. Saenz, and C. Ocal, *Surf. Sci.* **143**, 342 (1984).

⁴H. J. Simon, D. E. Mitchell, and J. G. Watson, *Phys. Rev. Lett.* **33**, 1531 (1974).

⁵Yu. E. Lozovik, S. P. Merkulova, M. M. Nazarov, and A. P. Shkurinov, *Phys. Lett. A* **276**, 127 (2000).

⁶M. J. Feldstein, P. Vohringer, W. Wang, and N. F. Scherer, *J. Phys. Chem.* **100**, 4739 (1996).

⁷Ulrich D. Keil, Taekjip Ha, Jacob R. Hensen, and Jorn M. Hvam, *Appl. Phys. Lett.* **72**, 3074 (1998).

⁸N. Del Fatti and F. Vallee, *Appl. Phys. B: Lasers Opt.* **73**, 383 (2001).

⁹M. Scharte, R. Porath, T. Ohms, M. Aeschlimann, J. R. Krenn, H. Ditlbacher, F. R. Aussenegg, and A. Liebsch, *Appl. Phys. B: Lasers Opt.* **73**, 305 (2001).

¹⁰N. García, I. G. Saveliev, and M. Sharonov, *Philos. Trans. R. Soc. London, Ser. A* **360**, 1039 (2002).

¹¹C. J. Powell and J. B. Swan, *Phys. Rev.* **118**, 640 (1960).

¹²K. E. Oughstun and H. Xiao, *Phys. Rev. Lett.* **78**, 642 (1997).

¹³P. B. Johnson and R. W. Christy, *Phys. Rev. B* **6**, 4370 (1972).

¹⁴E. Kretschmann and H. Raether, *Z. Naturforsch. A* **23**, 2135 (1968).

¹⁵Fadi I. Baida, Daniel Van Labeke, and J. M. Vigoureux, *Phys. Rev. B* **60**, 7812 (1999).

¹⁶P. Dawson, F. de Fornel, and J.-P. Goudonnet, *Phys. Rev. Lett.* **72**, 2927 (1994).

¹⁷B. Lamprecht, J. R. Krenn, G. Schider, H. Ditlbacher, M. Salerno, N. Felidj, A. Leitner, F. R. Aussenegg, and J. C. Weeber, *Appl. Phys. Lett.* **79**, 51 (2001).